A&A 502, 355–365 (2009)
DOI: 10.1051/0004-6361/200811527

Astronomy & Astrophysics

The distant activity of the Long Period Comets C/2003 O1 (LINEAR) and C/2004 K1 (Catalina)⋆

E. Mazzotta Epifani[1], P. Palumbo[2], M. T. Capria[3], G. Cremonese[4], M. Fulle[5], and L. Colangeli[1]

[1] INAF-Osservatorio Astronomico di Capodimonte, via Moiariello 16, 80131 Napoli, Italy
e-mail: epifani@na.astro.it
[2] Universitá Parthenope, Dip. Scienze Applicate, Centro Direzionale Isola C4, 80143 Napoli, Italy
[3] INAF-Istituto di Astrofisica Spaziale, via del Fosso del Cavaliere 100, 00133 Roma, Italy
[4] INAF-Osservatorio Astronomico di Padova, vicolo dell'Osservatorio 5, 35122 Padova, Italy
[5] INAF-Osservatorio Astronomico di Trieste, via Tiepolo 11, 34131 Trieste, Italy

Received 16 December 2008 / Accepted 7 April 2009

ABSTRACT

Aims. We study the distant dust environment of two Long Period Comets: C/2003 O1 (LINEAR) (observed at r_h = 7.39 AU) and C/2004 K1 (Catalina) (observed at r_h = 3.43 AU). The case of C/2003 O1 is particularly interesting since the comet has a quite large perihelion heliocentric distance (r_h = 6.85 AU).
Methods. We analysed *R*-band images taken at the CAHA 2.2 m telescope to characterise the properties of the cometary dust coma. The images of both comets were also used as input into an inverse numerical model, to derive information about the dynamical parameters of coma dust grains until a time ~500 days before the observation.
Results. Both the comets appeared to be active, and of similar shape and size despite the great difference in their heliocentric distance of observation. C/2003 O1 exhibited a tail extending to at least 3.7×10^5 km. It is a very active object, since its A$f\rho$ is 552 ± 36 cm within the inner 5″. C/2004 K1 showed a similar long tail, extending to 2.6×10^5 km. Its A$f\rho$ is 539 ± 35 cm within the inner 5″. An almost constant dust grain ejection velocity between 0.5 and 0.9 m/s at 1 cm dust size has been derived for C/2003 O1 and an increase from 0.5 to 2 m/s at 1 cm dust size for C/2004 K1, reflecting the different volatile dragging the dust environment (probably CO for C/2003 O1 and water for C/2004 K1). Model results allow some speculations about the comet nucleus size of C/2003 O1 (LINEAR) and its CO content: for a Q_{CO} similar in value to those observed for other distant cometary objects, a comet radius R_n from 13 to 17 km can be inferred.

Key words. comets: individual: C/2003 O1 (LINEAR) and C/2004 K1 (Catalina) – comets: general

1. Introduction

The observation of comets at large distances from the Sun can provide important information about the dynamics, collisions, and physical and chemical conditions in the early solar nebula. Meech & Hainout (2001) discussed extensively the importance of observing distant comets and how the information gathered could help in investigating the processes of formation and evolution of planetesimals (collisional accretions, size distribution, chemical conditions) at different heliocentric distances in the primordial solar nebula.

It is now widely accepted that cometary nuclei originate in at least two different regions of the solar system, implying that physical properties should be diverse because of differences in e.g. collisional environment, chemical composition of the primordial nebula, and radiation processing, etc. Based on the present Tisserand parameter (with respect to Jupiter), the classification scheme proposed by Levison (1996) distinguishes between Ecliptic Comets (EC) ($2 \leq T_J \leq 3$) and Nearly Isotropic Comets (NIC) ($T_J < 2$). The first family has a quasi-correspondance with the group of Short Period Comets (SPC). The second family includes both the Halley-type comets and the Long Period Comets. Following the definition of Lamy et al. (2005), the population of the NICs is further divided into two subgroups: the Dynamically New Comets (DNC), with original semi-major axis $a \geq 10^4$ AU, which are on their first passage in the solar system, and the returning NICs, that have already passed in the solar system, which typically have $a \leq 10^4$ AU. Originating in-situ in the Uranus-Neptune zone, ECs are thought to be collisional fragments of Kuiper Belt Objects, while the NICs probably formed in the region of giant planets (the Jupiter-Neptune zone) and then scattered towards the Oort cloud region.

There is much reference in the literature to "new" comets (i.e., comets that rarely pass through the Solar System) being intrinsically more active at large distances from the Sun than the periodic ("old") comets (i.e., comets for which many passages inside the Solar System have been recorded). The first extensive analysis in this field was summarised by Meech (1991), but at that time too few observations of cometary nuclei at large heliocentric distances (R > 3–4 AU, e.g., beyond the region where H_2O ice activity is expected to dominate) were available to make a conclusive claim. Meech (1988) presented an observational program for 28 comets belonging to different dynamical families and discussed the greater activity of dynamically new comets (e.g., an extensive coma for comet C/1984 W2 (Hartley) at r_h = 8.5 AU and for comet C/1980 E1 (Bowell)

⋆ Based on observations collected at the Centro Astronómico Hispano Alemán (CAHA) at Calar Alto, operated jointly by the Max-Planck Institute für Astronomie and the Instituto de Astrofísica de Andalucia (CSIC).

at r_h = 13.6 AU) with respect to periodic targets (e.g., comet 9P/Tempel 1 presenting an asteroidal light curve from recovery until about r_h = 2.4 AU). The chemical and physical aging effects on cometary nuclei have also been studied (Meech 1999) in terms of their different role and consequence for different dynamical cometary families, resulting in significant differences in the amount of outgassing between DNCs and SPCs, and a more uniform activity along the orbit in new comets, a larger surface area being available for gas sublimation due to lack of mantling.

Several long-term programs have been developed to observe from the ground (mostly visible imaging) a huge number of SPCs at large heliocentric distances, to perform an extensive analysis of the nuclear properties of this family, such as magnitude, shape, rotational status, albedo, and size (Meech et al. 2004; Licandro et al. 2000; Lowry et al. 1999; Lowry & Fitzsimmons 2001, 2005; Lowry et al. 2003; Lowry & Weissman 2003; Mazzotta Epifani et al. 2007, 2008). Two extensive works (Lamy et al. 2005; Tancredi et al. 2006) collected all the data available on SPCs from these systematic surveys, to investigate the nucleus size distribution and the cumulative luminosity function within the family. In contrast, a relative small number of studies have been devoted until now to analyse the distant properties of Long Period Comets. A summary of the analysis of the distant environment of comets pertaining to this family is presented in Table 1.

The distant activity of 20 LPCs, where r_h at the observation ranges from 3.35 to 19.4 AU (with the exceptional case of comet C/1995 O1 observed at $r_h \sim 26$ AU), has been studied in more or less detail by several methods. The majority of information comes from visible photometry, by which the morphology of the coma, general dust characteristics such as the A$f\rho$ parameter and $V - R$ colour, and estimates of the nuclear diameter can be derived. For some of the brightest comets, a visible spectrum has been derived for the coma, obtaining interesting information about unusual richness in CO^+ (Korsun et al. 2006), even if the low spectral resolution leaves some doubts about the line identification, or distant detection of C_3 (Rauer et al. 2003), both depicting a scenario of CO-rich comets. The advent of the IR space telescope *SPITZER* allowed us to investigate the IR environment of a distant LPC (C/2001 HT50 (LINEAR-NEAT), Kelley et al. 2006), and analyse its relative mineralogy. In one only case, for comet C/1995 O1 (Hale-Bopp), the distant dust environment of a LPC has been analysed by means of a numerical dust model, to derive detailed information about the dust grain ejection velocity, dust-loss rate and size distribution of particles (Fulle et al. 1998). The main results in terms of image analysis (integrated magnitude, A$f\rho$ parameter) obtained for the distant comets listed in Table 1 are summarised in Table 2.

The main aim of our work is to contribute to the field of ground-based investigation of the dust environment of distant LPCs, by means of the detailed analysis of two LPCs: C/2003 O1 (LINEAR) and C/2004 K1 (Catalina). The orbital parameters of the two objects are summarised in Table 3.

C/2003 O1 (LINEAR) was discovered in July 2003 in the course of the LINEAR (Lincoln Near-Earth Asteroid Research) project (Kusnirak & Birtwhistle 2003). It is a hyperbolic comet of perihelion distance quite distant from the Sun (r_h = 6.85 AU). The integration of its orbit to compute its original orbital parameters (in particular, $1/a$) shows that the target is not a strictly "new" comet (e.g., this has not been its first passage close to the Sun). The observations presented in this paper were performed after its last passage at perihelion.

C/2004 K1 (Catalina) was discovered by the Catalina Sky Survey in May 2004, initially classified as an asteroid and shortly after identified as exhibiting a weak coma (Spahr et al. 2004). It is classified as a returning Nearly Isotropic Comet, with a quite large semi-major axis (a = 1816 AU) and a close perihelion distance (r_h = 3.40 AU). The observations presented in this paper were performed shortly before its perihelion passage.

Section 2 describes the observations performed in May 2005. The analysis of the obtained *R*-band images is presented in Sect. 3. In Sect. 4 the possible sources of cometary distant activity are discussed, while in Sect. 5 the theoretical model applied to the images is described. The results of the model application to the comet images are described in Sect. 6. In Sect. 7, we discuss the implications of the obtained results for comet C/2003 O1 (LINEAR) for the determination of its nucleus size and the analysis of its volatile content. Summary and conclusions are given in Sect. 8.

2. Observations and reduction

The two comets C/2003 O1 (LINEAR) and C/2004 K1 (Catalina) were observed on May 15, 2005 with the 2.2 m telescope at the Centro Astronómico Hispano Alemán (CAHA) at Calar Alto (Spain). The images were obtained with the CAFOS (Calar Alto Faint Object Spectrograph) instrument, equipped with the 2k × 2k SITE#1d CCD with 24 μm pixels (pixel scale of 0.53 arcsec/px) and the Cousin broadband filter *R*.

In both cases, several long (>300 s) exposures were obtained for the object, during which the telescope tracking at the non-sidereal rate corresponded to the predicted motion of the comets. All the images were bias-subtracted and flat-fielded in the standard manner using the ESO Munich Image Data Analysis System, MIDAS (1998). The bias value was obtained using zero-second exposure bias frames. A flat field was created averaging several twilight sky exposures.

For comet C/2003 O1 (LINEAR), we obtained 3 long-exposure consecutive images of 1 × 1200 s and 2 × 900 s. For comet C/2004 K1 (Catalina), we obtained 3 long-exposure consecutive images of 2 × 600 s and 1 × 300 s. The two comets were easily identificable and appeared active in all the single exposures.

To improve the SNR for the image analysis, we decided to coadd the single images for each comet. The position of the comet optocentre in each single image selected for coadding was determined by fitting a two-dimensional Gaussian to the innermost 80 and 36 pixels of the coma images of comet C/2003 O1 (LINEAR) and C/2004 K1 (Catalina), respectively. The images were then recentred using this optocentre and summed. Sky correction was performed by subtracting a first-order polynomial sky approximation computed from the pixel areas containing no stars. The observing conditions are summarised in Table 4. The final images are reported in Figs. 1 and 2.

To perform an absolute flux calibration of the comet images, appropriate fields from the list of Landolt (1992) (SA104 350, PG1530, and PG1633) were observed at different airmasses during the observation night. The night was photometric, the seeing value, which was measured as the average FWHM of several sample stars from individual short-exposure frames, being stable around 1.9″.

3. Image analysis

3.1. Comet C/2003 O1 (LINEAR)

Despite the large heliocentric distance at the time of observation, the comet C/2003 O1 (LINEAR) (Fig. 1) reveals a very

Table 1. Summary of analysis of the distant environment of Long Period Comets.

Comet	r_h^a	Type of analysis	Reference
C/1980 E1 (Bowell)	13.6	Broadband CCD photomety	Meech (1988)
C/1983 O1 (Cernis)	13.2	Broadband CCD photomety	Meech (1988)
	17.4	Broadband CCD photomety	Meech (1990)
	19.4	Broadband CCD photomety	Meech (1992)
C/1984 K1 (Shoemaker)	8.6	Broadband CCD photomety	Meech (1988)
C/1983 W2 (Hartley)	8.5	Broadband CCD photomety	Meech (1988)
C/1986 P1 (Wilson)	5.0	Broadband CCD photomety	Meech (1988)
C/1995 O1 (Hale-Bopp)	13–4 Pre	Analysis of the dust tail by means of the inverse dust tail model	Fulle et al. (1998)
	4.6–2.9 Pre; 2.8–12.8 Post	Optical (longslit spectra and images) long-term monitoring	Weiler et al. (2003); Rauer et al. (2003)
	25.8 Post	VR_c photometry	Szabó et al. (2008)
C/1999 F2 (Dalcanton)	5.51	V and R photometric analysis	Szabó et al. (2001)
C/1999 J2 (Skiff)	7.14	VR photometric analysis	Szabó et al. (2001)
	7.24	IF390 and RX filters photometric analysis; modelling of the dust tail	Korsun & Chorny (2003)
	7.11 Pre–10.1 Post	VRI photometry	Meech et al. (2009)
C/1999 N4 (LINEAR)	5.51	VR photometric analysis	Szabó et al. (2001)
C/1999 T2 (LINEAR)	3.35	VR photometric analysis	Szabó et al. (2001)
C/2000 H1 (LINEAR)	3.89	VR photometric analysis	Szabó et al. (2001)
C/2000 K1 (LINEAR)	6.43	VR photometric analysis	Szabó et al. (2001)
C/2000 SV74 (LINEAR)	4.24	vgrz (Gunn) photometric analysis; CN, CO+ and C_2 spectrophotometry	Szabó et al. (2002)
C/2001 G1 (LONEOS)	8.32 Pre - 11.22 Post	$BVRI$ photometry	Meech et al. (2009)
C/2001 HT50 (LINEAR-NEAT)	4.60	SPITZER IR images and spectra	Kelley et al. (2006)
C/2001 Q4 (NEAT)	5.84	VRI photometry	Meech et al. (2009)
	8.60	Vis imaging and spectroscopy	Tozzi et al. (2003)
C/2002 T7 (LINEAR)	3.52	NIR spectroscopy	Kawakita et al. (2004)
C/2002 VQ94 (LINEAR)	6.80	Vis photometry and long-slit spectroscopy	Korsun et al. (2006)
C/2003 A2 (Gleason)	11.49 Pre–13.97 Post	VRI photometry	Meech et al. (2009)
C/2003 O1 (LINEAR)	7.02 Pre–8.18 Post	VRI photometry	Meech et al. (2009)

[a] Heliocentric distance (AU) of observation. Pre: pre-perihelion. Post: post-perihelion.

active object with a well-developed coma and a long tail extending in the E direction. The coma is slightly asymmetric: it extends (counts above 1σ of the background) to 3.7×10^4 km in the S and in the W directions and to 2.6×10^4 km in the N direction. The projected length of the tail (measured along the E direction) is at least 3.7×10^5 km (counts above 1σ of the background).

The R magnitudes of the comet, derived in different optical apertures centred on the optocentre, are summarised in Table 5. In the inner $5''$, the integrated R magnitude is 18.51 ± 0.07. The final uncertainity in the comet magnitude was derived from the photometric error $\sigma_{\rm calib}$ in the calibration curve, taken as the rms of the weighted standard stars fit.

Table 2 summarises the information about the integrated R magnitudes of Long Period Comets available until now. Little data are available, and direct comparison does not seem easy. For example, compared to C/1999 J2 (Skiff), observed at a rather similar heliocentric distance, comet C/2003 O1 (LINEAR) may be interpreted to be darker in the R band, but unfortunately we have no indication of the aperture value used by those authors to derive the magnitude, so a precise and direct comparison is impossible.

The reduced R magnitude of the comet can be computed as

$$H_R(1,0,0) = R - 5\log(r_h\Delta) - 0.04\alpha, \quad (1)$$

where r_h is the heliocentric distance, Δ the geocentric distance, and α is the phase angle during the observations (°). Values for comet C/2003 O1 (LINEAR), derived in different optical apertures centred on the optocentre, are listed in Table 5. Meech et al. (2009) measured the reduced R magnitude of comet C/2003 O1 (LINEAR) at three dates between 7.02 AU preperihelion and 8.18 AU postperihelion, obtaining values from 11.379 (July 23, 2003 – Preperihelion) to 11.649 (Aug. 16, 2004) to 12.735 (Feb. 07, 2006). Our value of 10.177 (measured for a comparable photometric aperture on May 15, 2005) seems to indicate a brighter object with respect to those measurements. A possible reason for this discrepancy could be a rotational modulation, but unfortunately we do not have enough data to assess the problem in a more accurate way.

A proxy for the dust production is the A$f\rho$ value (cm) (A'Hearn et al. 1984), where A is the average grain albedo, f the filling factor in the aperture field of view, and ρ the linear radius of the aperture at the comet, i.e. the sky-plane radius. Interpreted to be the percentage of solar radiation scattered by the cometary dust towards the observer, A$f\rho$ can be derived from the calculated photometric magnitude

$$Af\rho = \frac{4 \cdot r_h^2 \cdot \Delta^2 \cdot 10^{0.4(m_S - m_C)}}{\rho} \quad (2)$$

where m_S is the Sun magnitude in the R band and m_C is the R magnitude of the comet in an aperture of radius ρ.

Values of A$f\rho$ for C/2003 O1 (LINEAR), in different aperture radii, are given in Table 5. In the inner $5''$, the computed A$f\rho$ is 552 ± 36. A monotonic decrease in A$f\rho$ values with the nucleocentric distance ρ may be indicative of non-steady-state dust emission and possibly dust grain fading or destruction, as reported for several comets such as C/2000 WM1 (LINEAR) (Lara et al. 2004) and C/2001 Q4 (NEAT) (Tozzi et al. 2003).

Table 2. Summary of available results from image analysis of Long Period Comets.

Comet	r_h^a	$\log_{10}\rho$ (km)^b	$m_R{}^c$	A$f\rho$ (cm) ^{d}	Reference
C/1999 T2 (LINEAR)	3.35	?	15.9		Szabó et al. (2001)
C/2000 H1 (LINEAR)	3.89	3.9	19.7	38‡	Szabó et al. (2001)
C/2000 SV74 (LINEAR)	4.04	2	15.3	1892	Szabó et al. (2002)
C/1995 O1 (Hale-Bopp)	4–13			3×10^3 - $8 \times 10^4{}^e$	
C/1999 N4 (LINEAR)	5.5	?	18.8†		Szabó et al. (2001)
C/1999 F2 (Dalcanton)	5.51	4.07	19.1	172‡	Szabó et al. (2001)
C/2000 K1 (LINEAR)	6.43	?	18.4†		Szabó et al. (2001)
C/2003 O1 (LONEOS)	7.02–8.18	§	11.37–12.9$^\#$	1.3×10^3 - 318	Meech et al. (2009)
C/1999 J2 (Skiff)	7.14	?	17.7†		Szabó et al. (2001)
	7.11–10.1	§	9.9–13.4$^\#$	4.7×10^3 - 234	Meech et al. (2009)
C/2001 Q4 (NEAT)	8.6	4		1500	Tozzi et al. (2003)
	5.84	§	13.11$^\#$	304	Meech et al. (2009)
C/2001 G1 (LONEOS)	8.32–11.22	§	11.1–14.2$^\#$	1.8×10^3 - 28	Meech et al. (2009)
C/2003 A2 (Gleason)	11.49–14.04	§	11.6–12.8$^\#$	1.2×10^3 - 407	Meech et al. (2009)
C/1995 O1 (Hale-Bopp)	13	5.3		3×10^4	Weiler et al. (2003)
C/1983 O1 (Cernis)	19.4	?	23		Meech (1992)
C/1995 O1 (Hale-Bopp)	25.8	?	20		Szabó et al. (2008)

^{a} Heliocentric distance (AU) of observation. ^{b} Linear radius of the reference aperture at the comet. The symbol § corresponds to values by Meech et al. (2009) computed all using a 3.0″ radius photometric aperture. ^{c} Integrated R magnitude in the reference aperture. † Indicates a value obtained as the mean of the given light curve. # Indicates the average reduced R magnitude for $r = \Delta = 1$ and $\alpha = 0°$. ^{d} ‡ Indicates that the value is not given by the respective authors in the reference, but it has been computed for this paper with their data by means of Eq. (2) (see text). ^{e} Derived from a theoretical model.

Table 3. Orbital parameters of the target comets.

Comet	a (AU)^a	q (AU)^b	t_p^c	e^d	P (year)^e	Peri (°)^f	Node (°)^g	i (°)^h
C/2003 O1 (LINEAR)	−4902.61	6.847	2004 Mar. 17	1.001	–	81.62	347.64	117.98
C/2004 K1 (Catalina)	1816.25	3.399	2005 Jul. 5	0.998	7.74×10^4	97.75	326.92	153.74

^{a} Semimajor axis. ^{b} Perihelion distance. ^{c} Time of perihelion passage. ^{d} Orbital eccentricity ^{e} Orbital period. ^{f} The J2000 argument of perihelion. ^{g} The J2000 longitude of the ascending node. ^{h} Inclination.

Table 4. Observing conditions.

Comet	Observation time (UT)^a	r (AU)^b	Δ (AU)^c	α (°)^d	PA (^{o}) ^{e}	Total exposure time ^{f}	Airmass^g
C/2003 O1 (LINEAR)	2005 May 16 02:13	7.39	6.89	9.96	180.3	3000	1.094
C/2004 K1 (Catalina)	2005 May 15 23:51	3.43	2.57	10.3	204.3	1500	1.139

^{a} UT time in the middle of the total exposure time (coadded image). ^{b} Heliocentric distance. ^{c} Geocentric distance. ^{d} Sun-target-observer angle. ^{e} Position angle of the extended Sun-target radius vector. ^{f} Resulting from coadding of the individual frames. ^{g} In the middle of the total exposure time (coadded image).

In contrast, for an ideal steady-state coma, A$f\rho$ should be constant at all apertures. Values of C/2003 O1 (LINEAR), reported in Table 5, differ slightly for different cometocentric distances, but the values are compatible within the measurements errors. Therefore, we can conclude that the dust environment of C/2003 O1 (LINEAR), derived from analysis of coma photometry, is consistent with a scenario of steady-state emission.

Little data are available for A$f\rho$ for distant LPCs, as summarised in Table 2. The A$f\rho$ for our target (observed at r_h = 7.39 AU) is of the same order of magnitude as that obtained for the second target presented in this paper (see sect. below), observed at a much lower heliocentric distance. Meech et al. (2009) measured the A$f\rho$ for C/2003 O1 (LINEAR) at two values of heliocentric distances (r_h = 6.92 and 8.18 AU postperihelion) bracketing our value at r_h = 7.39 AU. The overall behaviour of A$f\rho$ is that (expected) of a decrease with increasing heliocentric distance, reflecting a general decrease in the dust activity.

Our results for comet C/2003 O1 (LINEAR) indicate a significant dust production rate, and support the idea that LPCs are far more active than SPCs along the entire orbit and especially at large heliocentric distance (Meech 1988). For example, A$f\rho$ = 195 cm for P/2002 T5 (LINEAR) observed at 5.24 AU (Mazzotta Epifani et al. 2008), and A$f\rho$ = 13 cm for P/1998 U4 (Spahr) observed at 6.14 AU (Lowry & Fitzsimmons 2005).

3.2. Comet C/2004 K1 (Catalina)

Observed at r_h = 3.43 AU, comet C/2004 K1 (Catalina) is not really a "distant" object, but results for this comet are interesting because few data are available for LPCs. Figure 2 shows a very active object with a well-developed coma and a long tail extending in the S-E quadrant. The coma is only slightly asymmetric: it extends (counts above 1σ of the background) to 2.1×10^4 km in the N direction and up to 2.61×10^4 km in the W direction. The projected length of the tail (measured along a direction perpendicular to the PA of the comet, which is 204.3°) is at least 2.6×10^5 km (counts above 1σ of the background) .

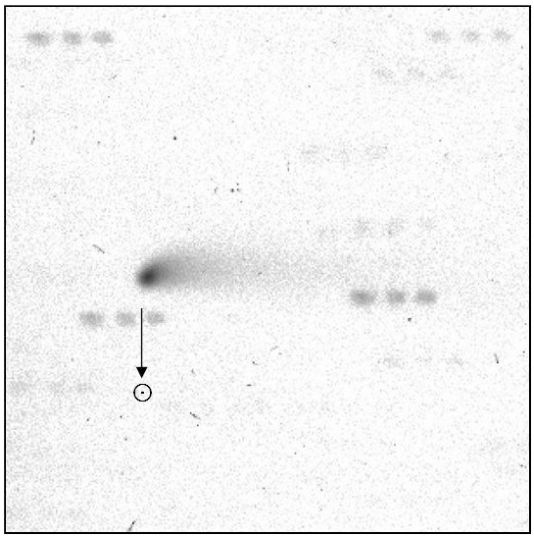

Fig. 1. Composite image of comet C/2003 O1 (LINEAR). The image width is 82 × 82 arcsec^2. The grey scale is logarithmic. N is down, E is right. The PA of the comet is 180.3°.

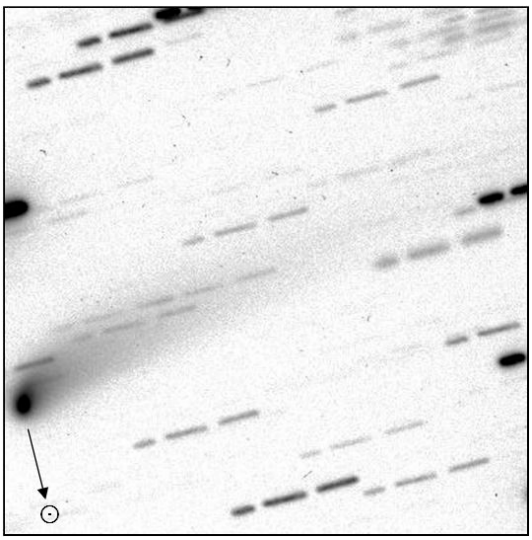

Fig. 2. Composite image of comet C/2004 K1 (Catalina). The image width is 110 × 110 arcsec^2. The grey scale is logarithmic. N is down, E is right. The PA of the comet is 204.3°.

The R magnitudes of the comet, derived in different optical apertures centred on the optocentre, are summarised in Table 5. In the inner 5″, the integrated R magnitude is 15.80 ± 0.07. The final uncertainity in the comet magnitude was derived from the photometric error $\sigma_{\rm calib}$ in the calibration curve, taken to be the rms of the weighted fit to standard stars. By comparison with data in Table 2, we can conclude that comet C/2004 K1 (Catalina) is a rather "standard" comet in terms of brightness: at almost the same heliocentric distance, C/1999 T2 (LINEAR) (Szabó et al. 2001) and C/2000 SV74 (LINEAR) (Szabó et al. 2002) exhibit similar integrated magnitudes.

For different aperture radii, values of A$f\rho$ for C/2004 K1 (LINEAR) are shown in Table 5. In the inner 5″, the computed A$f\rho$ is 539 ± 35. Figure 3 shows a clear monotonic decrease in A$f\rho$ values with the nucleocentric distance ρ, possibly indicative of non-steady-state dust emission and dust grain fading or destruction, as reported for several comets such as C/2000 WM1 (LINEAR) (Lara et al. 2004) and C/2001 Q4 (NEAT) (Tozzi et al. 2003).

Also A$f\rho$ data for C/2004 K1 (LINEAR) support the idea that LPCs are far more active than Short Period Comets along the whole orbit (Meech 1988): SPCs observed at the same heliocentric distance exhibit A$f\rho$ values an order of magnitude lower than that measured for our target: for example, 48 cm for 139P/Väisälä-Oterma (Lowry & Fitzsimmons 2001), 75 cm for 119P/Parker-Hartley (Lowry et al. 1999), and 49 cm for 103P/Hartley 2 (Mazzotta Epifani et al. 2008).

4. Source of cometary distant activity

The primary driver of activity in comets close to the Sun is sublimation of H_2O ice, but there is debate about the cause of activity at heliocentric distances too far and too cold for significant water sublimation. Calculations of gas production for sublimation from different volatiles indicate that the sublimation rate for H_2O ice decrease significantly beyond a heliocentric distance of $r_{\rm h}$ = 3 AU. Sublimation of H_2O ice could be sufficient to lift observable dust grains from the cometary surface and account for the development of a dust coma out to 5–6 AU (Meech & Svoren 2005). Activity beyond this distance could be caused by the perihelion heat wave penetrating into the volatile-rich depths in the nucleus (Meech & Svoren 2005), but the discovery of active comets that have likely not been close to the Sun enough (or ever) to experience heating (as for example C/2003 O1 (LINEAR)) implies that a different mechanism exists. For these comets, the distant activity could be explained more accurately by the sublimation or the release of very volatile gases, in particular CO and/or CO_2.

It is widely believed that highly volatile material froze on the surface of cometesimals in the outer regions of the presolar nebula in which comets formed (Notesco et al. 2003). In cometary nuclei CO has been observed to be quite abundant (as high as 24% relative to water in some comets) (Bockelée-Morvan et al. 2005), but it is still unclear whether these highly volatile materials are present in so significant amounts as pure ice in the cometary nucleus to sustain (by sublimation) various degrees of activity. In this case, the activity could begin at significant distances from the Sun, since the CO ice sublimation begins at 25 K, corresponding to $r_{\rm h} \sim 120$ AU. In contrast, models and simulations performed on the SPCs and the few observed LPCs showed that CO and other volatiles can be present in the cometary nuclei as gases trapped in the cells of amorphous water ice and that a significant release of gas can occur when the irreversible transition from amorphous to crystalline state takes place, at temperatures around 90 K (Prialnik et al. 2005), corresponding to $r_{\rm h} \sim 11$ AU. In this case, the trapped gas could be of relatively high abundance: water ice has the ability to trap gases up to a gas-to-ice ratio of 3.3, as seen in laboratory experiments (Laufer et al. 1987).

Cometary activity along the comet's orbit, and in particular at large heliocentric distances (often characterised by outbursts, erratic activity in periodic comets, and unusually high coma brightness), has been studied by several groups from a theoretical point of view, compiling reliable mathematical models of both the thermal evolution and the differentiation inside the nucleus and simulating the structure and the evolution of the comet nucleus itself (Tancredi et al. 1994; Coradini et al. 1997; Julian et al. 2000; Gutiérrez et al. 2001; Capria 2002; Cohen et al. 2003; Prialnik et al. 2005). All the nucleus models attempt to solve the heat transport and the gas diffuse equations in the nucleus by assuming different levels of symmetry and

Table 5. Magnitude and A$f\rho$ of the target comets.

Comet	$d(")^a$	R	$H_R(1,1,0)$	$\log_{10}\rho$ (km)^b	A$f\rho$ (cm)
C/2003 O1 (LINEAR)	2.65	19.11 ± 0.07	10.177	4.14	572 ± 37
	4.77	18.51 ± 0.07	9.577	4.40	552 ± 36
C/2004 K1 (Catalina)	2.65	16.35 ± 0.07	11.212	3.82	585 ± 38
	4.77	15.80 ± 0.07	10.662	4.07	539 ± 35
	6.89	15.53 ± 0.07	10.392	4.23	479 ± 31
	9.54	15.33 ± 0.07	10.192	4.37	416 ± 27

[a] Aperture diameter. [b] Linear radius of the aperture at the comet.

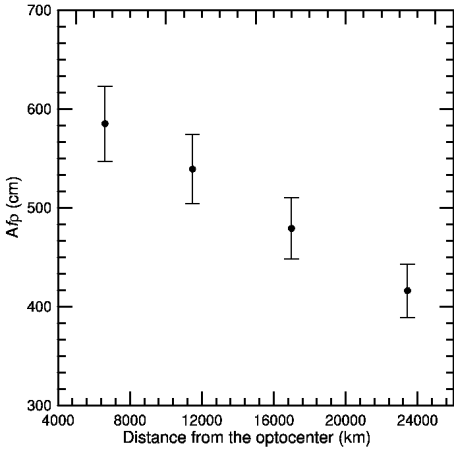

Fig. 3. A$f\rho$ for comet C/2004 K1 (LINEAR) computed from photometric magnitude at different nucleocentric distance, as derived from Eq. (2) (see text).

sphericity, and depicting the nucleus as a porous object composed of a mixture of dust and different ices. For comet C/1995 O1 (Hale-Bopp), the observed activity and volatile production rate over a wide range of heliocentric distances was well reproduced by a numerical model (Capria et al 2000).

The results of the models in terms of CO outgassing and production rate show that for CO both in a pure ice and in a trapped gas form, the source of a CO-driven activity should be beneath the surface, where the internal temperatures could drop quickly to very low values. Another characteristic of CO-driven activity that can be derived from the theoretical models is that CO, when present, tends to flow from the body along most of its orbit and from everywhere on the surface, due to the low sublimation temperature and the depth of the sublimation and transition fronts. The sublimation front, in particular, should be at a quasi-constant temperature.

The dust release from the nucleus surface caused by CO drag is then expected to differ from that due to water, i.e., CO, and its associated dust flux, are expected to leave the comet nucleus uniformly from all the nucleus surface, on both the night and day sides. Since it originates from the nucleus interior, its loss rate is also expected to change very slowly with time after the onset of activity.

5. The numerical dust tail model

The theoretical fitting of the observed tail cannot be achieved with a direct dust-tail model, i.e., changing all possible input parameters and determining which provides the closest fit, because the high number of parameters in every realistic dust model implies that hundreds of different parameter combinations, not necessarily similar, would provide fits of similar quality. Therefore, to fit the observed cometary tails and reconstruct the dust environment of the two comets and its time evolution starting from the observation and going back in time, we adopted a regularized inverse approach that ensures we reach the most probable fit (with a least squares criterium). This approach characterises the inverse dust-tail model, extensively described in Fulle (1989) and Epifani et al. (2001). Here we briefly recall only that the approach consists of two main steps: (i) computing the model dust tail; and (ii) fitting this to the observed tail to derive the dust parameters. The solution of the fit gives sampled values of the dust loss rate, $\dot{M}(t)$, the size distribution $n(d,t)$, and A$f\rho$. Other non-linear parameters must be determined by a trial-and-error procedure:

(i) the dust ejection velocity, $v(t,d_0)$, which describes the time evolution of the dust ejection, where t is the time of dust ejection from the inner coma and d_0 a reference diameter;
(ii) the power index, $u = \partial \log v(t,d)/\partial \log d$, which characterises the power-law dependence of the dust velocity on the grain diameter d: $v(t,d) = v(t,d_0)\cdot(d/d_0)^u$;
(iii) the dust ejection anisotropy parameter, w, which is the half width of the Sun-pointing dust ejection cone, where $w = 180°$ means isotropic emission, $w = 90°$ stands for emispherical emission, and $w = 45°$ means strongly anisotropic emission.

This approach allows us to reduce significantly the number of tests necessary to ensure the uniqueness of the output parameter combination, because all the linear parameter are automatic outputs of the code, and only combinations of non-linear parameters must be investigated. Since the time-dependent dust loss rate and the time and size-dependent dust distribution are linear parameters of the model, the uniqueness of the output is stabler than in every direct approach. In the inverse approach, only the time- and size-dependent dust ejection velocity vector must be found by means of a trial-and-error procedure. Therefore, this quantity must be constrained by physical considerations, independent of the dust tail model, which we can derive taking into account considerations discussed in Sect. 4.

6. Results for observed comets

6.1. Comet C/2003 O1 (LINEAR)

Figure 4 shows isophotes of the CAHA image of comet C/2003 O1 (LINEAR) (panels *a* to *f* refer to different *(u, w)* combinations, see Sect. 5 for details). Figure 5 shows the time evolution in the cometary dust environment, as derived from the modelling of the CAHA image (Fig. 4, dashed isophotes). The results cover a time span from a heliocentric distance r_h = 7.01 AU pre-perihelion to the date of observation (r_h = 7.39 AU post-perihelion). As discussed in Sect. 4, the rather large perihelion distance of the comet C/2003 O1 (LINEAR) implies that water

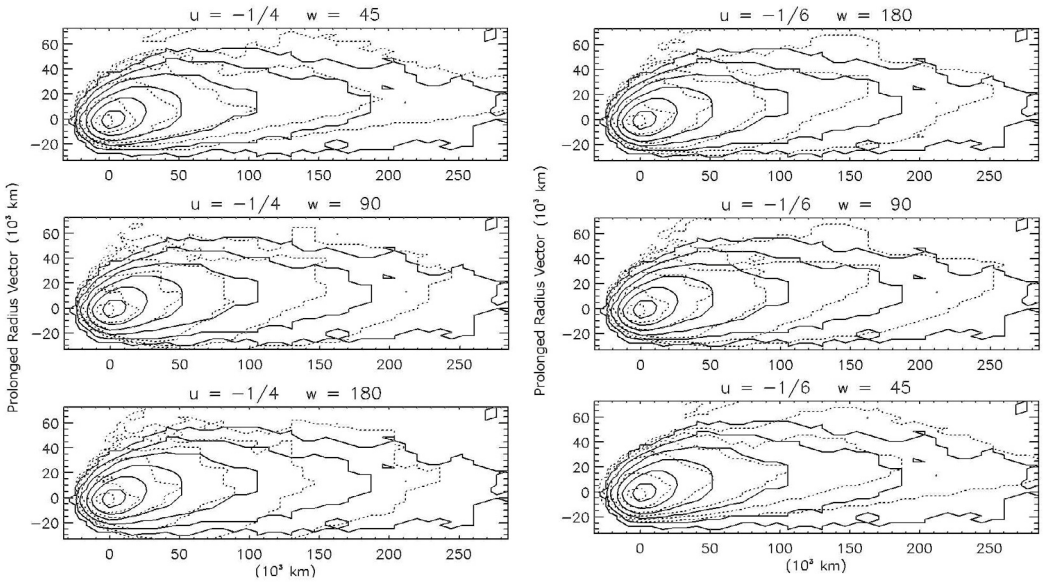

Fig. 4. Observed (continuous lines) and calculated (dashed lines) isophotes of comet C/2003 O1 (LINEAR). The innermost isophote corresponds to 23.8 R-mag arcsec^{-2}. The isophote step is 0.75 R-mag arcsec^{-2}. The Sun-pointing sky-projected vector is towards bottom. The different panels refer to different *(u, w)* combinations (see text for more details).

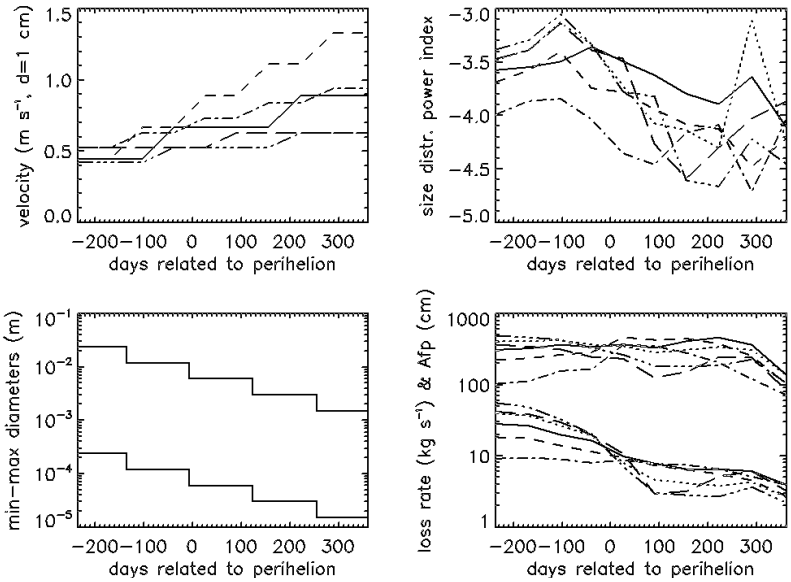

Fig. 5. Dust environment of comet C/2003 O1 (LINEAR) derived from the modelling of the CAHA image. Dust ejection velocity (*upper left*), power index of the differential size distribution (*upper right*), size interval to which all the shown outputs are related (*lower left*), mass-loss rate, and A$f\rho$ values (*lower right*). The line styles refer to different sets of parameters: $u = -1/6$ and $W = 180°$ (continuous line); $u = -1/6$ and $W = 90°$ (dotted line); $u = -1/6$ and $W = 45°$ (short dashed line); $u = -1/4$ and $W = 180°$ (long dashed line); $u = -1/4$ and $W = 90°$ (three dots-dashed line); $u = -1/4$ and $W = 45°$ (dot-dashed line).

should provide a negligible contribution to dust drag in the coma. Assuming that most of the gas released along the orbit (and responsible for the cometary activity) is CO, with an approximately constant loss rate and speed, and isotropic distribution, we should select in Fig. 5 the solutions that match this hypothesis more closely.

Panel *a* shows the time evolution in the dust ejection velocity. Its size-dependence is tested by the u parameter: $u = -1/2$ is expected for perfectly spherical grains, $u > -1/2$ is expected for more and more aspherical grains, and $u = -1/6$ is the upper limit to all results obtained by means of photometric analysis of dust tails. Many inverse tail model applications have shown that dust tail brightness data are unable to constrain the u parameter uniquely. Changes in the outputs related to different u input values allow us to estimate the uncertainty affecting the model solutions. We indeed find that isotropic solutions ($w = 180°$), with aspherical grains, provide an almost constant ejection velocity, of between 0.5 and 0.9 m/s for 1 cm dust grain size.

Panel *c* of Fig. 5 shows which time-dependent β parameter range allows us to fit the observed dust tail. We have already

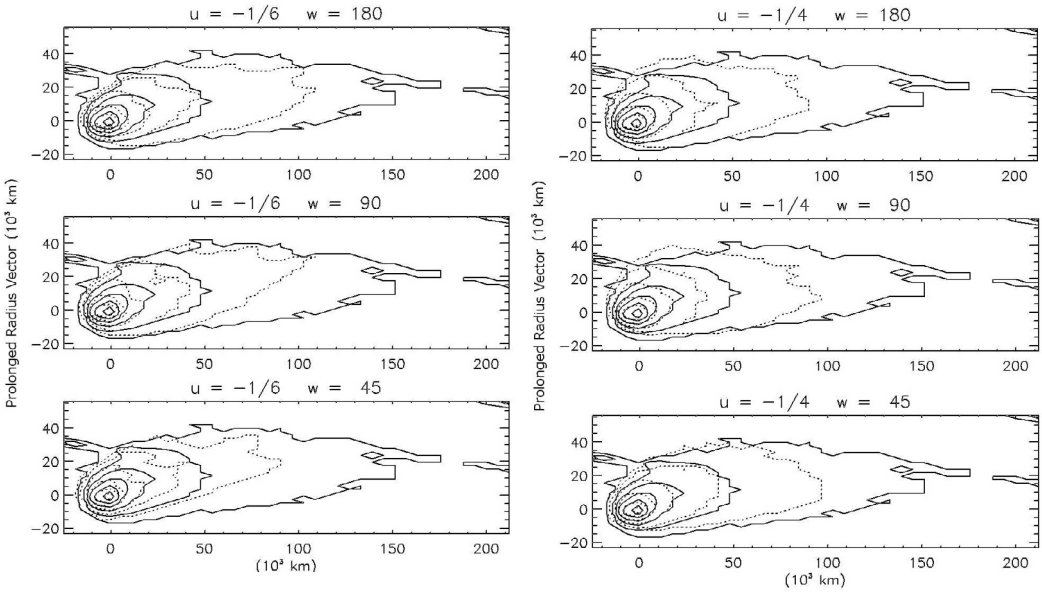

Fig. 6. Observed (continuous lines) and calculated (dashed lines) isophotes of comet C/2004 K1 (Catalina). The innermost isophote corresponds to 20.9 *R*-mag arcsec^{-2}. The isophote step is 0.75 *R*-mag arcsec^{-2}. The Sun-pointing sky-projected vector is towards bottom. The different panels refer to different *(u, w)* combinations (see text for more details).

converted the β parameter in sizes, by means of Eq. (3) (for more details, see for example Krishna Swamy 1986)

$$\beta = \frac{C_{\rm pr} Q_{\rm pr}}{\rho_{\rm d} d} \qquad (3)$$

where $C_{\rm pr}$ (depending on light velocity, solar mass, and G) is equal to 1.19×10^{-3} kg m^{-2} and $Q_{\rm pr}$ is the dust scattering efficiency of grains of diameter d and bulk density $\rho_{\rm d}$. In this conversion, a dust bulk density of 10^3 kg m^{-3} was adopted, and an increased value of the dust bulk density would provide a corresponding decrease in dust size. Moreover, a dust scattering efficiency $Q_{\rm pr} = 1$ was adopted, as being probable for absorbing grains. A different value for $Q_{\rm pr}$ would relate to corresponding variation in size. Of course, dust grains of size outside the range shown in Fig. 4 was also ejected from the inner coma, but smaller grains are outside the image in Fig. 4, while larger grains fall in the nucleus pixel of Fig. 4. This panel of Fig. 5 suggests that all the observed tail must consist of grains larger than 0.1 mm, if the dust bulk density is 10^3 kg m^{-3}.

Panel *d* shows the time evolution in the dust mass loss rate. This value comes out a factor of ten lower than that obtained by the same inverse dust tail model applied to the active Centaur P/2004 A1 (LONEOS) (Mazzotta Epifani et al. 2006), decreasing from 30 kg/s before perihelion to about 4 kg/s shortly before the observations. The most probable explanation of this decrease is a systematic change in the size distribution along the orbit, whose mean power-index time evolution is shown in panel *b*. The mean power-index decreases from about −3.5 (dust mass dominated by the largest ejected grains) to values lower than −4 (dust mass dominated by the smallest grains scattering light in the coma). Since dust ejection driven by CO is presumably isotropic, such long-term changes cannot be due to seasons of the nucleus, as is well known, for example, for the SPC 2P/Encke (Epifani et al 2001). A more consistent explanation is given by inhomogeneities in the dust population at different nucleus depths, i.e., before perihelion layers with a slightly larger population of large grains were ejected. After perihelion, CO started to drag dust from lower nucleus layers with a mean dust population slightly depleted of these large grains.

Panel *d* of Fig. 5 also provides the A$f\rho$ values that are consistent with the dust models that reproduce most closely the observed dust tail. Since the dust model considers a limited dust size range (see panel *c*), the model can only predict lower limits to the A$f\rho$ observed values. Shortly before the observations, the model infers A$f\rho \sim 2$ m, which is consistent with the observed value of 5.5 m.

6.2. Comet C/2004 K1 (Catalina)

Figure 6 shows isophotes of the CAHA image of comet C/2004 K1 (Catalina) (panels *a* to *f* refer to different *(u, w)* combinations, see Sect. 5 for details). Figure 7 shows the time evolution in the cometary dust environment, as derived from the modelling of the CAHA image (Fig. 6, dashed isophotes). The results cover a time span between the time coresponding to a heliocentric distance of $r_{\rm h} = 6.51$ AU pre-perihelion and the date of observation ($r_{\rm h} = 3.43$ AU pre-perihelion). As discussed in Sect. 4, the perihelion distance of comet C/2004 K1 (Catalina) is consistent with classic dust drag by water, and therefore all solutions of the dust tail model should provide a $r_{\rm h}$-dependent velocity. This is indeed the case: panel *a* of Fig. 7 shows that both isotropic ($w = 180°$) or anisotropic ($w = 45°$) ejections, during the two years before perihelion (~the time of present observations), require an increase in the dust velocity from 0.5 m/s to 1.5–2 m/s (at 1 cm dust size) to reproduce the observed dust tail, although the shape of the comet tail appears to be similar to that of comet C/2003 O1 (LINEAR).

Panel *c* of Fig. 7 shows which time-dependent β parameter range allows us to fit the observed dust tail, which has been converted into sizes (see Sect. 6.1). The same dust bulk density of 10^3 kg m^{-3} was adopted, and a dust scattering efficiency $Q_{\rm pr} = 1$, as is probable for absorbing grains. This panel of Fig. 7 suggests that all the observed tail must consist of grains

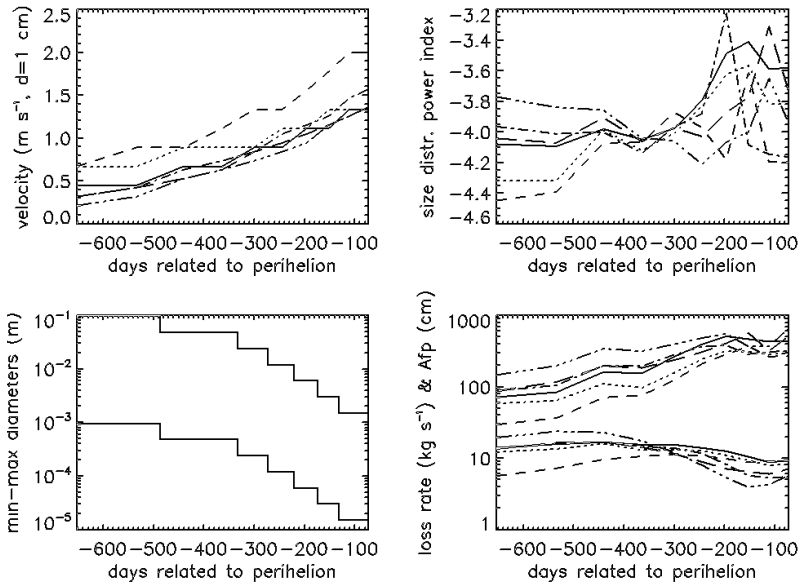

Fig. 7. Dust environment of comet C/2004 K1 (Catalina) derived from the modelling of the CAHA image. Dust ejection velocity (*upper left*), power index of the differential size distribution (*upper right*), size interval to which all the shown outputs are related (*lower left*), mass loss rate, and A*fρ* values (*lower right*). The line styles refer to different sets of parameters: $u = -1/6$ and $W = 180°$ (continuous line); $u = -1/6$ and $W = 90°$ (dotted line); $u = -1/6$ and $W = 45°$ (short dashed line); $u = -1/4$ and $W = 180°$ (long dashed line); $u = -1/4$ and $W = 90°$ (three dots-dashed line); $u = -1/4$ and $W = 45°$ (dot-dashed line).

larger than 0.1 mm if the dust bulk density is 10^3 kg m^{-3}, and also that slightly larger grains with respect to comet C/2003 O1 (LINEAR) (grain size ∼10 cm) are needed to fit the tail brightness distribution.

Panel *b* shows the time evolution in the dust size distribution for the comet. The time variation in the two years preceeding the observation is almost negligible, with values rising from -4.1 ± 0.3 two years before perihelion to -3.8 ± 0.4 shortly before perihelion. However, the uncertainty in these values is such that a constant dust size distribution seems consistent with the tail brightness distribution. As shown in panel *d*, the dust mass loss-rate indeed remains almost constant at 10 kg/s, while the A*fρ* value increased slightly from 1 to 4 m in the same two years, which is again consistent with the observed value of 5 m reported in Table 5.

7. C/2003 O1 (LINEAR) nucleus size and volatile content

Comet nucleus size distributions are of great interest because they preserve a record of the outer nebula mass distributions in the late stages of planetary formation, as well as a record of collisional evolution. In this sense, the differences in the size distribution between different cometary classes are crucial: Short-Period Comets are thought to be collisional fragments from the Edgeworth-Kuiper Belt population, injected into resonaces to form the present family (Davis & Farinella 1997). In contrast, Long-Period Comets that have been stored inside the Oort Cloud may not have been affected by collisions, so that their size distribution could be considered primordial.

The results of the dust model application to the image of comet C/2003 O1 (LINEAR) can be used to derive indirect information about the nucleus size of the target and its volatile content. The fit to the cometary isophote suggests that all the observed tail must consist of grains larger than 0.1 mm if the dust bulk density is 10^3 kg m^{-3}. Assuming that all of the dust rate is due to CO sublimation, this size allows us to infer the lower

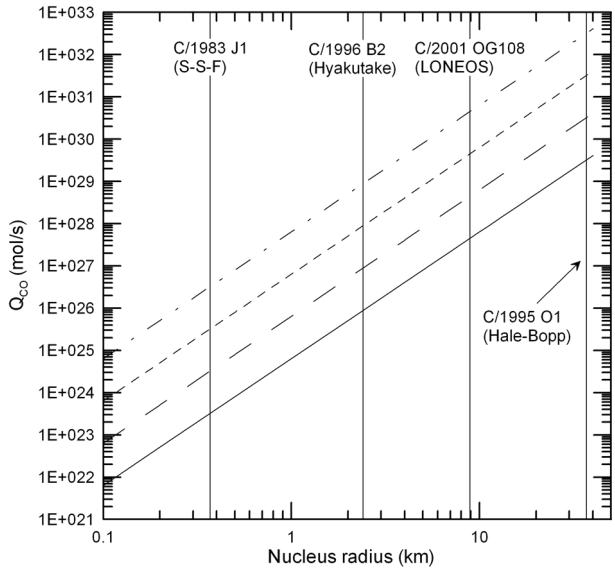

Fig. 8. CO production rate versus different cometary nucleus radius R_N, as derived from Eq. (4) (see text). Different curves corresponds to different maximum size a_{max} of grain lifted by the CO flux: 0.01 cm (continuous), 0.1 cm (long dashed), 1 cm (short dashed), 10 cm (dot-dashed). The vertical lines correspond to measured R_N for some LPCs.

value of the CO loss rate Q_{CO} necessary to lift this grain. For uniform outgassing, the (maximum) size of lifted grain is (Crifo 1999)

$$a_{max} = 1.57 \times 10^{-27} Q_{CO} R_n^{-3} \text{ cm} \quad (4)$$

where R_n is the radius of the nucleus (assumed to be a sphere). Equation (4) has been used to compute the curves of Fig. 8.

The few values of nucleus radius for LPCs available in literature have been recently summarised by Lamy et al. (2005): they range from a sub-km radius of $R_n = 0.37$ km for comet C/1983 J1 (Sugano-Saigusa-Fujikawa) (Hanner et al. 1987) to

R_n = 8.9 km for comet C/2001 OG108 (LONEOS) (Abell et al. 2003) and the large value of R_n = 37 km for the "giant" comet C/1995 O1 (Hale-Bopp) (Weaver & Lamy 1997). Since we do not have information about the nucleus of comet C/2003 O1 (LINEAR), we are only able to make realistic assumptions based on the possible CO production rate (as the probable driver of cometary activity) at large heliocentric distance.

To our knowledge, a direct measurement of the CO production at large heliocentric distances (>4–5 AU) is available for only a few comets (and even less for LPCs). Using data obtained from radio wavelength observations of the strongest CO transitions, Biver et al. (2002) summarised values for comet C/1995 O1 (Hale-Bopp) ($\sim 3 \times 10^{28}$ mol s^{-1} at r_h = 6 AU pre-perihelion, and $\sim 5 \times 10^{27}$ mol s^{-1} at r_h = 14 AU post-perihelion). At r_h = 7.4 AU post-perihelion (the heliocentric distance of the C/2003 O1 observations presented in this paper), they reported a value of $Q_{CO} \sim 2.5 \times 10^{28}$ mol s^{-1}. For the active Centaur 29P/Schwassmann-Wachmann, a $Q_{CO} \sim 3.5 \times 10^{28}$ mol s^{-1} was measured around r_h = 6 AU (Senay & Jewitt 1994; Crovisier et al. 1995; Festou et al. 2001). Womack & Stern (1999) derived a production rate of $Q_{CO} = 1.5 \pm 0.8 \times 10^{28}$ mol s^{-1} for the active Centaur (2060) Chiron, although this marginal detection has not been confirmed by independent observations (Rauer et al. 1997; Bockelée-Morvan et al. 2001). Only upper limits to the production rate have been derived for the LPC C/1999 J2 (Skiff) observed at r_h = 7.2 AU ($\leq 2 \times 10^{28}$ mol s^{-1}, Biver 2001) and for the active Centaur C/2001 T4 (NEAT) at r_h = 8.6 AU ($\leq 2.4 \times 10^{28}$ mol s^{-1}, Jewitt et al. 2008).

Although the Q_{CO} observed in distant cometary objects depends strongly on observational bias and heliocentric distance, we can summarise that a value in the range 1.5–3.5×10^{28} mol s^{-1} could be considered to be typical for a heliocentric distance ~6–8 AU. Considering the results of the dust-tail modelling of comet C/2003 O1 (LINEAR) (the fit to the cometary isophote suggests that all the observed tail must consist of grains larger than 0.1 mm if the dust bulk density is 10^3 kg m^{-3}, see Sect. 6.1), the results plotted in Fig. 8 infer, for a minimum Q_{CO} from 1.5 to 3.5×10^{28} mol s^{-1}, a cometary radius R_n from 13 to 17 km. For a dust bulk density of 3×10^3 kg m^{-3} (and therefore a minimum grain size of 3.3×10^{-3} mm in the tail), the inferred cometary nucleus radius would become even larger than 20 km. A smaller (and probably more realistic) value for the nucleus of C/2003 O1 (LINEAR) would imply (see Fig. 8) a quite low Q_{CO}: for R_n = 1 km we would obtain $Q_{CO} = 6.4 \times 10^{24}$ mol s^{-1}.

The amount of CO (relative to water) in comets observed until now is highly variable (from 0.4 to 24%, see Mumma et al. (2003) and Bockelée-Morvan et al. (2005), even if these [CO]/[H_2O] ratios are observed for non-distant comets, where a strong sublimation of water is established, so that these values could be close to the true abundances ratios of cometary ices). Therefore, the CO content in a cometary nucleus could reflect the different formation history of the nuclei (different regions in the nebula, e.g., different temperatures and condensation rate) (Hill et al. 2001), and this is particularly interesting in LPCs, which are understood to have formed elsewhere and then been scattered in the "storage" of the Oort Cloud. The detection of CO and the amount of CO outgassing in LPCs therefore provides an interesting clue to constrain the formation and evolution processes of minor bodies in the Solar System, considering also that for CO an extended source could also be present in the coma (Capria et al. 2000; Gunnarsson 2003; Gunnarsson et al. 2003), and we should distinguish between these two contributes.

8. Summary and conclusions

We have presented data for two Long Period Comets: C/2003 O1 (LINEAR) and C/2004 K1 (Catalina), observed at heliocentric distances larger than r_h = 3 AU. Both were active at time of observation, C/2003 O1 (LINEAR) in particular exhibiting significant activity at its very large heliocentric distance of r_h = 7.39 AU post-perihelion. We used the images as input to an inverse numerical model, to derive information on the physical parameters of dust grains in the coma and their time evolution.

Our main results can be summarised as follows:

1. Both the comets appeared to be active with a coma and a well-developed dust tail, and were similar in shape and size, despite the great difference in their heliocentric distances of observation. We observed C/2003 O1 (LINEAR) at r_h = 7.39 AU post-perihelion, where it exhibited a coma extending to at least 3.7×10^4 km in the S-W quadrant, and a long dust tail extending at least to a projected distance of 3.7×10^5 km. We observed C/2004 K1 (Catalina) shortly before its perihelion at r_h = 3.43 AU, where it exhibited a coma extending at least to 2.6×10^4 km in the N-W quadrant and a long tail extending to at least a projected distance of 2.6×10^5 km.
2. For comet C/2003 O1 (LINEAR), in the inner 5″ the integrated R magnitude is 18.51 ± 0.07 and the A$f\rho$ value is 552 ± 36 cm, indicative of a significant dust production rate even at large heliocentric distances. The A$f\rho$ value is constant at different nucleocentric distances ρ, in a way that is consistent with a scenario of steady-state emission.
3. For comet C/2004 K1 (Catalina), in the inner 5″ the integrated R magnitude is 15.80 ± 0.07 and the A$f\rho$ value is 539±35 cm. A clear monotonic decrease in A$f\rho$ values is visible for the nucleocentric distance ρ: this may indicate non-steady-state dust emission and possible dust grain fading or destruction inside the coma.
4. For comet C/2003 O1 (LINEAR), the application of the inverse numerical model has allowed the reconstruction of the time evolution in the dust ejection velocity for a time interval around the perihelion corresponding to heliocentric distances from 7.01 AU pre-perihelion to the distance at observing time. The velocity remains almost constant between 0.5 and 0.9 m/s for 1 cm dust size, which is consistent with a scenario of dust drag dominated by steady CO emission.
5. For comet C/2004 K1 (Catalina), the dust ejection velocity increased from 0.5 m/s at a heliocentric distance of 6.51 AU pre-perihelion to 2 m/s at the distance at observing time, which is consistent with a scenario of a classical r_h-dependent dust drag dominated by water in the inner part of the cometary orbit.
6. The dust mass loss-rate for C/2003 O1 (LINEAR) decreases from ~30 kg/s before perihelion to ~4 kg/s shortly before the observations. The most probable explanation of this decrease is the inhomogeneity in the dust population at different nucleus depths: before perihelion, layers with a slightly larger population of large grains were ejected. After perihelion, CO started to drag dust from lower nucleus layers that have a mean dust population slightly depleted of large grains.
7. The dust mass loss rate for C/2004 K1 (Catalina) remains almost constant at ~10 kg/s between 6.51 AU and 3.43 AU pre-perihelion.
8. Based on the isophote fitting by the model, all the observed tail of comet C/2003 O1 (LINEAR) must consist of grains larger than 0.1 mm if the dust bulk density is 10^3 kg m^{-3}. This allows us to speculate about the comet nucleus size

and its volatile (CO) content: for a minimum Q_{CO} of between 1.5 and 3.5×10^{28} mol s^{-1} (as for the only three distant cometary objects for which the CO outgassing has been measured), a comet radius R_n from 13 to 17 km can be inferred. In contrast, a smaller (and probably more realistic) value for the nucleus of C/2003 O1 (LINEAR) would result in a quite low Q_{CO}: for R_n = 1 km, we would obtain $Q_{CO} = 6.4 \times 10^{24}$ mol s^{-1}.

Acknowledgements. We warmly thank the referee (J. Crovisier) for his helpful comments on the paper, especially in the interpretation and discussion of cometary radio observations. Observations presented in this paper have been funded by the Optical Infrared Coordination Network (OPTICON), a major international collaboration supported by the Research Infrastructures Programme of the European Commission's Sixth Framework Programme. We also gratefully aknowledge funding from Italian Space Agency (ASI) under contract I/015/07/0.

References

Abell, P. A., Fernández, Y. R., Pravec, P., et al. 2003, in Lunar and Planetary Science XXXIV, Abstract 1253 (Houston: Lunar and Planetary Institute)
A'Hearn, M. F., Schleicher, D. G., Feldman, P. D., Millis, R. L., & Thompson, D. T. 1984, AJ, 89, 579
Biver, N. 2001, ICQ, 23, 85
Biver, N., Bockelée-Morvan, D., Colom, P., et al. 2002, EM&P, 90, 5
Bockelée-Morvan, D., Lellouch, E., Biver, N., et al. 2001, A&A, 377, 343
Bockelée-Morvan, D., Crovisier, J., Mumma, M. J., & Weaver, H. 2005, in Comets II, ed. M., Festou, H. U., Keller, & H. A., Weaver (Tucson: Univ. Arizona Press)
Capria, M. T. 2002, EM&P, 89, 161
Capria, M. T., Coradini, A., De Sanctis, M. C., & Orosei, R. 2000, A&A, 357, 359
Cohen, M., Prialnik, D., & Podolak, M. 2003, New Astron., 8, 179
Coradini, A., Capaccioni, F., Capria M. T., et al. 1997, Icarus, 129, 2, 317
Crovisier, J., Biver, N., Bockelée-Morvan, D., et al. 1995, Icarus, 115, 213
Crifo, J. F., Rodionov, A. V., & Bockelée-Morvan, D. 1999, Icarus, 138, 1, 85
Davis, D. R., & Farinella, P. 1997, Icarus, 125, 50
Epifani, E., Colangeli, L., Fulle, M., et al. 2001, Icarus, 149, 339
Festou, M. C., Gunnarsson, M., Rickman, H., et al. 2001, Icarus, 150, 140
Fulle, M. 1989, A&A, 217, 283
Fulle, M., Cremonese, G., & Bohm, C. 1998, AJ, 116, 1470
Gunnarsson, M. 2003, A&A, 398, 353
Gunnarsson, M., Bockelée-Morvan, D., Winniberg, A., et al. 2003, A&A, 402, 383
Gutiérrez, P. J., Ortiz, J. L., Rodrigo, R., & López-Moreno, J. J. 2001, A&A, 374, 326
Hanner, M. S., Newburn, R. L., Spinrad, H., & Veeder, G. J. 1987, AJ, 94, 1081
Hill, H. G. M., Grady, C. A., & Nuth, J. A., III, et al. 2001, PNASS, 98, 2182
Jewitt, D., Garland, C. A., & Aussel, H. 2008, AJ, 135, 400
Julian, W. H., Samarasinha, N. H., & Belton, M. J. S. 2000, Icarus, 144, 160
Kawakita, H., Watanabe, J., Ootsubo, T., et al. 2004, ApJ, 601, L191
Kelley, M. S., Woodward, C. E., Harker, D. E., et al. 2006, ApJ, 651, 1256
Korsun, P. P., & Chorny, G. F. 2003, A&A, 410, 1029
Korsun, P. P., Ivanova, O. V., & Afanasiev, V. L. 2006, A&A, 459, 977
Kusnirak, P., & Birtwhistle, P. 2003, IAU Circ., 8170
Krishna Swamy, K. S. 1986, Physics of comets (World Scientific Pub.)
Lamy, P. L., Toth, I., Fernández, Y. R., & Weaver, H. A. 2005, in Comets II, ed. M., Festou, H. U. Keller, & H. A., Weaver (Tucson: Univ. Arizona Press)
Landolt, A. U. 1992, AJ, 104, 1, 340
Lara, L.-M., Tozzi, G. P., Boehnhardt, H., DiMartino, M., & Schulz, R. 2004, A&A, 422, 717
Laufer, D., Kochavi, E., & Bar-Nun, A. 1987, Phys. Rev. B, 36, 9219
Levison, H. F. 1996, in Completing the Inventory of the Solar System, ed. T. W., Retting, & J. M., Hahn (San Francisco: ASP), ASP Conf. Ser., 107
Licandro, J., Tancredi, G., Lindgren, M., Rickman, H., & Gil Hutton, R. 2000, Icarus, 147, 161
Lowry, S. C., & Fitzsimmons, A. 2001, A&A, 365, 204
Lowry, S. C., & Fitzsimmons, A. 2005, MNRAS, 358, 641
Lowry, S. C., & Weissmann, P. R. 2003, Icarus, 164, 492
Lowry, S. C., Fitzsimmons, A., Cartwright, I. M., & Williams, I. P. 1999, A&A, 349, 649
Lowry, S. C., Fitzsimmons, A., & Collander-Brown, S. 2003, A&A, 397, 329
Mazzotta Epifani, E., Palumbo, P., Capria, M. T., et al. 2006, A&A, 460, 935
Mazzotta Epifani, E., Palumbo, P., Capria, M. T., et al. 2007, MNRAS, 381, 713
Mazzotta Epifani, E., Palumbo, P., Capria, M. T., et al. 2008, MNRAS, 390, 1, 265
Meech, K. J. 1988, BAAS, 20, 835
Meech, K. J. 1990, BAAS, 22, 1103
Meech, K. J. 1991, in Comets in the Post-Halley Era, ed. R. L., Newburn, Jr., M., Neugebauer, & J., Rahe (Kluwer Acad. Pub.)
Meech, K. J. 1992, BAAS, 24, 993
Meech, K. J. 1999, in Evolution and Source Regions of Asteroids and Comets, ed. J. Svoren, E. M., Pittich, & H., Rickman, Tatranská Lomnica Astron. Inst. Slovak Acad. Sci., Proc. IAU Coll., 173
Meech, K. J., & Hainaut, O. R. 2001, in Collisional Processes in the Solar System, ed. M. Y., Marov, & H., Rickman, ASSL, 261 (Dordrecht: Kluwer Acad. Pub.)
Meech, K. J., & Svoren, J. 2005, in Comets II, ed. M., Festou, H. U., Keller, & H. A., Weaver (Tucson: Univ. Arizona Press)
Meech, K. J., Hainaut, O. R., & Marsden, B. G. 2004, Icarus, 170, 463
Meech, K. J., Pittichova, J., Bar-Nun, A., et al. 2009, Icarus, in press [doi:10.1016/j.icarus.2008.12.045]
Mumma, M. J., DiSanti, M. A., Dello Russo, N., et al. 2003, Adv. Space Res., 31, 2563
Notesco, G., Bar-Nun, A., & Owen, T. C. 2003, Icarus, 162, 183
Prialnik, D., Benkhoff, J., & Podolak, M. 2005, in Comets II, ed. M., Festou, H.U., Keller, & H. A., Weaver (Tucson: Univ. Arizona Press)
Rauer, H., Biver, N., Crovisier, J., et al., 1997, Planet. Space Sci., 45, 799
Rauer, H., Helbert, J., Arpigny, C., et al. 2003, A&A, 397, 1109
Senay, M. C., & Jewitt, D. 1994, Nature, 371, 229
Spahr, T., Battat, J. B., Stoss, R., Sanchez, S., & Nomen, J. 2004, IAU Circ., 8343
Szabó, G. M., Csák, B., Sárneczky, K., & Kiss, L. L. 2001, A&A, 374, 712
Szabó, G. M., Kiss, L. L., Sárneczky, K., & Sziládi, K. 2002, A&A, 384, 702
Szabó, G. M., Kiss, L. L., & Sárneczky, K. 2008, ApJ, 677, L121
Tancredi, G., Rickman, H., & Greenberg, J. M. 1994, A&A, 286, 659
Tancredi, G., Fernandez, J. A., Rickman, A., & Licandro, J. 2006, Icarus, 182, 2, 527
Tozzi, G. P., Boehnhardt, H., & Lo Curto, G. 2003, A&A, 398, L41
Weaver, H. A., & Lamy, P. L. 1997, EM&P, 79, 17
Weiler, M., Rauer, H., Knollemberg, J., Jorda, L., & Helbert, J. 2003, A&A, 403, 313
Womack, M., & Stern, A. S. 1999, Astron. Vestn., 33, 187